Springer Earth System Sciences

Diego Kietzmann
Andrés Folguera *Editors*

Opening and Closure of the Neuquén Basin in the Southern Andes

Springer

Diego Kietzmann · Andrés Folguera
Editors

Opening and Closure of the Neuquén Basin in the Southern Andes

Springer

Tectono-Stratigraphic Evolution of the Atuel Depocenter During the Late Triassic to Early Jurassic Rift Stage, Neuquén Basin, West-Central Argentina

Florencia Bechis, Laura B. Giambiagi, Maisa A. Tunik, Julieta Suriano, Silvia Lanés and José F. Mescua

Abstract The Neuquén Basin presents an almost continuous record from the Late Triassic until the Paleocene, making it an excellent case study of the most relevant tectonic stages of southern South America during the Mesozoic. It was initiated in Late Triassic to Early Jurassic times as a continental rift basin in the context of a widespread extensional stage that affected western Gondwana and culminated with the break-up of the supercontinent. The Atuel depocenter is located in the northern sector of the Neuquén Basin. Its synrift and sag units are represented by Upper Triassic to Lower Jurassic siliciclastic marine and continental sedimentary rocks including the oldest marine deposits of the basin, of Late Triassic age. The depocenter infill has been deformed and exhumed during the Andean orogeny, being presently exposed in the northern sector of the Malargüe fold and thrust belt. In this review, we have integrated a large set of stratigraphic, sedimentologic, geochronologic, and structural data in order to unravel the tectono-sedimentary evolution of the Atuel depocenter and to evaluate the main controlling factors of the synrift stage. We analyzed data from the synrift units, such as facies and thickness distribution, sandstone provenance, detrital zircon geochronology data, kinematic data from outcrop-scale normal faults,

F. Bechis (✉)
Instituto de Investigaciones en Diversidad Cultural y Procesos de Cambio (IIDyPCa). Consejo Nacional de Investigaciones Científicas y Técnicas (CONICET). Universidad Nacional de Río Negro, Sede Andina. Mitre 630, San Carlos de Bariloche, Argentina
e-mail: florbechis@gmail.com

L. B. Giambiagi · J. Suriano · J. F. Mescua
Instituto Argentino de Nivología, Glaciología y Ciencias Ambientales (IANIGLA). Consejo Nacional de Investigaciones Científicas y Técnicas (CONICET), Centro Científico Tecnológico Mendoza. Av. Ruiz Leal s/n, Parque General San Martín, Mendoza, Argentina

M. A. Tunik
Universidad Nacional de Río Negro. CONICET. Instituto de Investigaciones en Paleobiología y Geología. Av. Roca 1242., General Roca, Argentina

S. Lanés
Cape Town, South Africa

J. F. Mescua
Facultad de Ciencias Exactas y Naturales, Universidad Nacional de Cuyo, Mendoza, Argentina

D. Kietzmann and A. Folguera (eds.), *Opening and Closure of the Neuquén Basin in the Southern Andes*, Springer Earth System Sciences,
https://doi.org/10.1007/978-3-030-29680-3_2

angular and progressive unconformities, and subsurface information. Reactivation of preexisting NNW-striking anisotropies under a regional NNE extension resulted in an oblique rift setting, which generated a bimodal distribution of NNW- and WNW-striking major normal faults. Reduced strain and stress tensors obtained from the kinematic and dynamic analysis of structural data show a complex heterogeneity that we interpreted as a result of local stress permutations due to the activity of the larger faults and to strain partitioning inside the Atuel depocenter. Sedimentologic and petrographic data revealed a complex evolution with strong lateral variations of the depositional environments during the synrift phase, which lasted from Rhaetian to Pliensbachian times. We identified several stages that were controlled by processes of initiation, propagation, growth, linkage, and deactivation of new and reactivated faults along the depocenter evolution, in combination with sea-level changes related to global eustatic variations. Sandstone provenance data suggest an important basin reorganization by the Toarcian, probably related to the initiation of the sag stage in this depocenter.

Keywords Neuquén Basin · Atuel depocenter · Oblique rift · Kinematic and dynamic analysis · Sedimentary provenance

1 Introduction

The Neuquén Basin is an oil-bearing back-arc extensional basin developed in the southwestern margin of the Gondwana continent and open to the Pacific at its western margin. It hosts an almost continuous record of Late Triassic to Paleocene age (Uliana et al. 1989; Legarreta and Uliana 1999), making it an excellent case study that registers the most relevant tectonic stages of southern South America during the Mesozoic. It began in the Late Triassic to Early Jurassic as a continental rift basin due to a widespread extensional stage at western Gondwana, which gave way to the break-up of the supercontinent and the subsequent opening of the South Atlantic Ocean (Uliana et al. 1989; Vergani et al. 1995; Franzese and Spalletti 2001).

The Neuquén Basin shows a particular triangular shape (Fig. 1), with a western sector that has been deformed by the shortening that has built the Southern Central Andes since the Late Cretaceous (Cobbold and Rosello 2003), obscuring the original distribution of synrift deposits and their structural controls. The southern sector is a wide rift basin, with a more evenly distributed deformation and a more than 4000 m thick succession of volcanic, volcaniclastic, and clastic synrift deposits (Gulisano 1981; Carbone et al. 2011). The northern sector is a narrow and localized rift basin, whose early synrift deposits are continental-marine, clastic-volcanic successions of more than 2000 m (Gulisano and Gutiérrez Pleimling 1994).

The basin has several depocenters, each one showing a particular set of structural and stratigraphic features. Some of their differences can be attributed to strongly varying volumes of volcanic deposits and to a probable diachronic evolution of the early synrift, climax, and sag phases during a eustatic sea-level rise (see

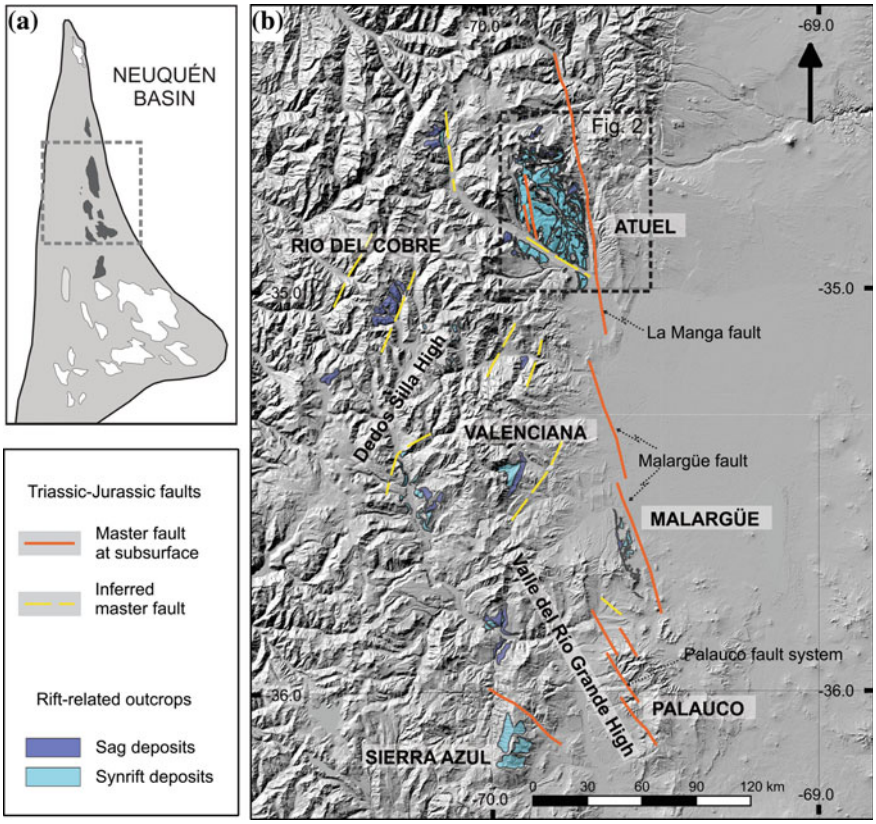

Fig. 1 Regional map showing the distribution of the principal normal faults and the infill of the Late Triassic to Early Jurassic synrift depocenters of the Neuquén Basin in the southern Mendoza province, west-central Argentina (modified from Manceda and Figueroa 1995; Yagupsky et al. 2008; Giambiagi et al. 2009a, b; Bechis et al. 2014; Mescua et al. 2014; Fuentes et al. 2016; Barrionuevo et al. 2019)

Chapter "The Syn-Rift of the Neuquén Basin-Precuyano and Lower Cuyano Cycle: Review of Structure, Volcanism, Tectono-Stratigraphy and Depositional Scenarios"). However, other controlling factors, such as the relative orientation of each depocenter respect to the regional stress field and the role of reactivated structures during the extensional event, have also been proposed (Vergani et al. 1995; Mosquera and Ramos 2006; Giambiagi et al. 2009a; Bechis et al. 2014).

The northern depocenters of the basin are the Yeguas Muertas, Nieves Negras, Atuel, Río del Cobre, Valenciana, Malargüe, Sierra Azul, and Palauco depocenters (Fig. 1; Gulisano and Gutiérrez Pleimling 1994; Manceda and Figueroa 1995; Giambiagi et al. 2009a). Firstly, during the Norian to Early Sinemurian, these depocenters were isolated by structural highs (e.g., Dedos-Silla High, Valle del

Rio Grande High, Manceda and Figueroa 1995), and later became progressively inter-connected during Sinemurian to Late Pliensbachian times.

The Atuel depocenter synrift and sag units are represented by Upper Triassic to Lower Jurassic siliciclastic marine and continental sedimentary rocks (Reijenstein 1967; Volkheimer 1978; Riccardi et al. 1991; Lanés 2005, Lanés et al. 2008), which host the oldest marine deposits of the basin, of Late Triassic age (Riccardi et al. 1997). Those successions have been deformed and exhumed during the Andean orogeny, and they presently crop out in the northern sector of the Malargüe fold and thrust belt (Kozlowski et al. 1993), making the Atuel depocenter one of the best study areas of the early stages of the Neuquén Basin development.

A number of sedimentological (Lanés 2002, 2005; Giambiagi et al. 2005a; Spalletti et al. 2007; Lanés et al. 2008; Tunik et al. 2008, 2011), structural (Giambiagi et al. 2005a, 2008a; Bechis, 2009; Bechis et al. 2009, 2010), and geochronological contributions (Naipauer et al. 2015; Horton et al. 2016) about the Atuel depocenter have been published in the last years. However, an integrated and multidisciplinary analysis of the available information has not been made so far. In this review, we have integrated the large set of available data in order to unravel its tectono-sedimentary evolution and to determine the main controlling factors of the synrift stage.

2 Tectonic Setting

The basement of the Neuquén Basin is affected by structures and rheological contrasts inherited from previous tectonic stages (Mosquera and Ramos 2006; Bechis et al. 2014; Mescua et al. 2016). The early Paleozoic geological evolution of this sector of Gondwana was determined by the accretion of Pampia, Cuyania, Chilenia, and Patagonia allochthonous terranes (Ramos et al. 1986; Ramos 1988, 2008; Astini et al. 1995; Rapalini 2005; Pankhurst et al. 2006; Varela et al. 2011; Tomezzoli 2012; Pángaro and Ramos 2012; see discussion and references therein). These collisions were later followed by the onset of a classical Andean-type margin associated with retroarc basins during the Carboniferous to Early Permian (Limarino and Spalletti 2006), which gave place to the Gondwana orogeny (Keidel 1916), locally known as San Rafael compressional phase (Azcuy and Caminos 1987; Mpodozis and Ramos 1989).

From the Late Permian to the Early Cretaceous, the region underwent extensional conditions, associated with the initial break-up of Gondwana (Charrier 1979; Llambías et al. 1993). The early stages were characterized by a widespread silicic magmatism of Late Permian to Early Triassic age, represented by the upper section of the Choiyoi Group (Llambías 1999; Sato et al. 2015; Giambiagi and Martínez 2008; Kleiman and Japas 2009). During the Early to Middle Triassic, this magmatism was progressively followed by the opening of several NNW-trending narrow continental rift systems, such as the Cuyo, Ischigualasto, and other coeval basins (Charrier 1979; Uliana et al. 1989; Kokogian et al. 1993; Japas et al. 2008; Giambiagi et al. 2011; Espinoza et al. 2018). Younger stages of rifting took place during the Middle to Late

Triassic in the Domeyko Basin (Espinoza et al. 2018) and during the Late Triassic to Early Jurassic in the Neuquén, Ramada, and other coeval basins, which formed new depocenters not geographically connected with the earlier ones (Alvarez and Ramos 1999; Charrier et al. 2007).

Since the late Early Jurassic, the southwestern margin of Gondwana was characterized by active subduction and a well-developed Andean magmatic arc (Mpodozis and Ramos 1989; Charrier et al. 2007), which was probably already active during the Triassic to Early Jurassic extensional stage (Llambías et al. 2007; Schiuma and Llambías 2008; Oliveros et al. 2018) (see Chapter "Early Andean Magmatism in Southern Central Chile, 33°–40° S"). Some authors argued that the regional extensional regime continued until the Early Cretaceous, related to the retreat of the Pacific trench (Mpodozis and Ramos 1989; Ramos and Kay 2006; Ramos 2010). From the Middle Jurassic onwards, the Neuquén Basin was subjected to thermal subsidence (Legarreta and Uliana 1996; Vergani et al. 1995; Howell et al. 2005). Then a second synrift stage is proposed during the Late Jurassic (Vergani et al. 1995; Giambiagi et al. 2003a; Charrier et al. 2007; Mescua et al. 2008) (see Chapter "Controls on Deposition of the Tordillo Formation in Southern Mendoza (34°–36° S): Implications for the Kimmeridgian Tectonic Setting of the Neuquén Basin"). At this time, local episodic shortening phases with selective inversion were registered in the southern sector of the basin during the Jurassic, mainly in the Huincul High (Vergani et al. 1995; Pángaro et al. 2006; Mosquera and Ramos 2006; Silvestro and Zubiri 2008; Cristallini et al. 2009).

Then, Andean uplift started in the Late Cretaceous (Cobbold and Rossello 2003; Zapata and Folguera 2005; Zamora Valcarce et al. 2006; Tunik et al. 2010; García Morabito and Ramos 2012; Mescua et al. 2013; Balgord and Carrapa 2016; Fennell et al. 2017; Gómez et al. 2019), with a renewed pulse of deformation and uplift from the Miocene to Recent (Giambiagi et al. 2003b, 2008b, 2014; Spagnuolo et al. 2012; Orts et al. 2012, Horton et al. 2016). During these shortening phases, the infill of the Neuquén Basin was deformed and exhumed giving way to thick-and thin-skinned fold and thrust belts on the western sector of the basin (Manceda and Figueroa 1995; Uliana et al. 1995; Zapata et al. 1999; Giambiagi et al. 2005b, 2008b; Zapata and Folguera 2005; Zamora Valcarce et al. 2006).

3 The Northern Neuquén Basin

The Late Triassic to Early Jurassic extensional architecture of the northern sector of the Neuquén Basin is made up by a set of NNW and NNE elongated depocenters with highly variable synrift thicknesses, including both continental volcaniclastic deposits and interbedded marine and continental siliciclastic facies (Fig. 1). The structure and infill of most of the depocenters of this sector are outlined in this section, while the main stratigraphic and structural characteristics of the Atuel depocenter are further described and discussed in the following sections.

Deposition of clastic continental synrift deposits (Remoredo Formation) in the **Sierra Azul depocenter** was controlled by movement along its NW-striking and SW-dipping master fault, El Manzano fault (Yagupsky et al. 2008). North of this fault, the basement rocks are covered by Upper Toarcian to Bajocian nearshore and offshore sag deposits (Gulisano and Gutiérrez Pleimling 1994). Toward the east, the **Palauco depocenter** was filled with volcaniclastic and volcanic deposits of the Precuyo Cycle (Gulisano 1981) or Precuyo Mesosequence (Legarreta and Gulisano 1989). Two NNW-striking and ENE-dipping master faults, the Los Cerrillos fault (Barrionuevo et al. 2019) and the Palauco fault (Manceda and Figueroa 1995; Giambiagi et al. 2009a), controlled the space creation within this depocenter. Immediately to the north, the **Malargüe depocenter** was controlled by the NNW-striking, WSW-dipping Malargüe normal fault, interpreted from seismic data (Silvestro and Kraemer 2005; Giambiagi et al. 2009a). Its synrift deposits (Tronquimalal Group; Stipanicic 1979) are clastic and volcaniclastic facies of humid alluvial fans and braided rivers interbedded with lacustrine black shales and sandstones (Spalletti 1997; Artabe et al. 1998; Buchanan et al. 2017) of Late Triassic age based on its paleofloristic content (Artabe et al. 1998). Here, the sag phase is represented by Bajocian nearshore marine deposits (Gulisano and Gutiérrez Pleimling 1994).

The **Valenciana depocenter** was filled with siliciclastic shallow nearshore to offshore marine deposits (Puesto Araya and Tres Esquinas Formations, respectively) with abundant Early Pliensbachian to Aalenian ammonites (Gulisano and Gutiérrez Pleimling 1994). Two tuffs from the lower portion of the Tres Esquinas Formation have been dated in 180.59 ± 0.43 and 181.42 ± 0.24 Ma (U/Pb in zircon; Mazzini et al. 2010). Fuentes et al. (2016) located its probable master fault through the location of the basement-synrift interface derived from well data. This master fault is a NNE-striking, WNW-dipping structure parallel to the Valenciana anticline axis, suggesting either the tectonic inversion of the previous normal fault or a strong control of this structure over the Cenozoic contractional structures.

The **Río Grande depocenter** was developed immediately to the west of the Valenciana depocenter. It was filled with ignimbrites and co-ignimbrite air-fall tuffs interbedded with lacustrine deposits (Lanés and Salani 1998; Lanés and Palma 1998) and overlain by Lower Toarcian–Lower Bajocian marine sediments (Westermann and Riccardi 1982; Damborenea 1987). According to Lanés and Salani (1998), these pyroclastic deposits are synchronic with the Cerro Negro Andesite dated with a crystallization zircon age of 223.3 ± 1.9 Ma (Naipauer et al. 2015). Based on palinspastically restored isopach maps, Manceda and Figueroa (1995) inferred a N to NNE-striking, eastward-facing listric master fault.

The **Los Blancos depocenter**, situated immediately to the south of the Rio del Cobre depocenter, is filled with continental and siliciclastic marine synrift deposits. Their basal portions correspond to sandstones and conglomerates deposited in a gravel braided fluvial system of Hettangian?—Sinemurian age (El Freno Formation; Lanés et al. 2013) in sharp or normal fault contact with basement rocks. Fluvial deposits are overlain by marine siltstone beds deposited in a shallow marine littoral environment with Late Sinemurian? to Early Toarcian ammonites, bivalves and brachiopods (Damborenea 1987) and black shales representing a quick relative sea-level

rise during the Toarcian (Gulisano and Gutiérrez Pleimling 1994). This depocenter is inferred to be controlled by the west-dipping, NNE-striking, Los Blancos fault (Mescua et al. 2014; Fuentes et al. 2016).

The **Río Del Cobre depocenter** has been interpreted as controlled by a NNE-trending master fault (Mescua et al. 2014). Its infill is characterized by a succession of 800 m of turbiditic sandstones, limestones, and shales with *Posidonomya alpina* and *Harpocerates* sp. (Gerth 1925), indicating an Early to Middle Jurassic age. Slumps and flute marks suggest a western provenance, consistent with the interpretation of W-sourced proximal submarine fans of the equivalent Nacientes del Teno Formation, cropping out westwards in Chile (Davidson 1988). Based on the fossil content, a correlation with the Puesto Araya and Tres Esquinas Formations of the Atuel depocenter has been proposed (Gulisano and Gutiérrez Pleimling 1994).

4 Stratigraphic Setting for the Atuel Depocenter

The structural basement of the Neuquén Basin in the Atuel depocenter area mainly comprises Permian to Triassic volcanic and plutonic rocks of the Choiyoi Group and a minor amount of Paleozoic metasedimentary rocks of the Las Lagunitas Formation and Carboniferous plutons such as the Carrizalito Tonalite (Fig. 2; Volkheimer 1978; Llambías et al. 1993; Sruoga et al. 2005; Nullo et al. 2005; Tickyj et al. 2009). These units crop out on blocks limited by deep-rooted reverse faults, like in the southernmost sector of the Frontal Cordillera north of the Atuel depocenter, on the Dedos-Silla High, and in the Malargüe and Bardas Blancas anticlines to the south (Figs. 1 and 2; Manceda and Figueroa 1995; Dicarlo and Cristallini 2007; Giambiagi et al. 2012; Mescua et al. 2014). In the Malargüe anticline, zircons from an ignimbrite assigned to the Choiyoi Group yielded a weighted mean U-Pb LA-ICP-MS age of 244.5 ± 2.0 Ma (Fig. 3; Horton et al. 2016). Basement rocks have also been localized in the subsurface to the east of the Atuel depocenter, where boreholes cut the entire sedimentary pile reaching its base (Bechis et al. 2010; Fuentes et al. 2016).

The Late Triassic to Early Jurassic infill of the Atuel depocenter consists of siliciclastic marine and continental sedimentary rocks, included in the Arroyo Malo, El Freno, Puesto Araya, and Tres Esquinas Formations (Fig. 2; Reijeinstein 1967; Stipanicic 1969; Volkheimer 1978; Riccardi et al. 1991, 1997; Gulisano and Gutiérrez Pleimling 1994; Lanés 2005; Lanés et al. 2008; Spalletti et al. 2007). These units have been assigned to the lower Cuyo Group (Stipanicic 1969; Gulisano 1981; Legarreta and Gulisano 1989; Riccardi and Damborenea 1993), although part of this sequence is coetaneous with the Precuyo Cycle or Mesosequence (Gulisano 1981; Legarreta and Gulisano 1989). This stratigraphic section is exposed to the west of the Borbollón–La Manga lineament, a conspicuous NNW-striking structure that extends for more than 50 km along the northeastern sector of the Malargüe fold and thrust belt (Giambiagi et al. 2005a). Exhumation of these deposits was associated with an important denudation, probably favored by the inversion of the Mesozoic normal faults during the Andean shortening (Giambiagi et al. 2012). Conversely, eastwards

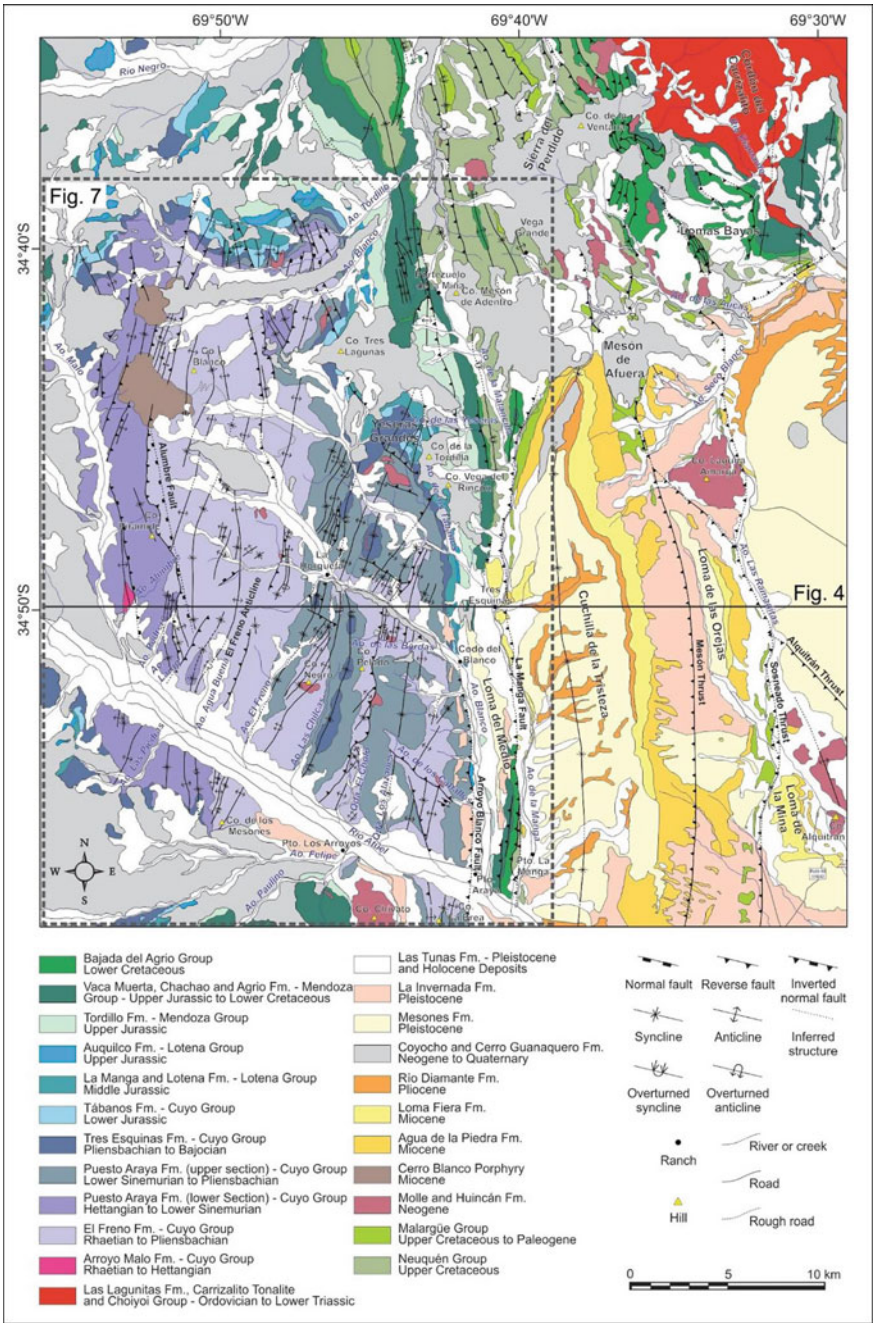

Fig. 2 Geologic map of the studied area, located in the northeastern sector of the Malargüe fold and thrust belt (modified from Giambiagi et al. 2008b; Bechis 2009; and references therein). See location map on Fig. 1

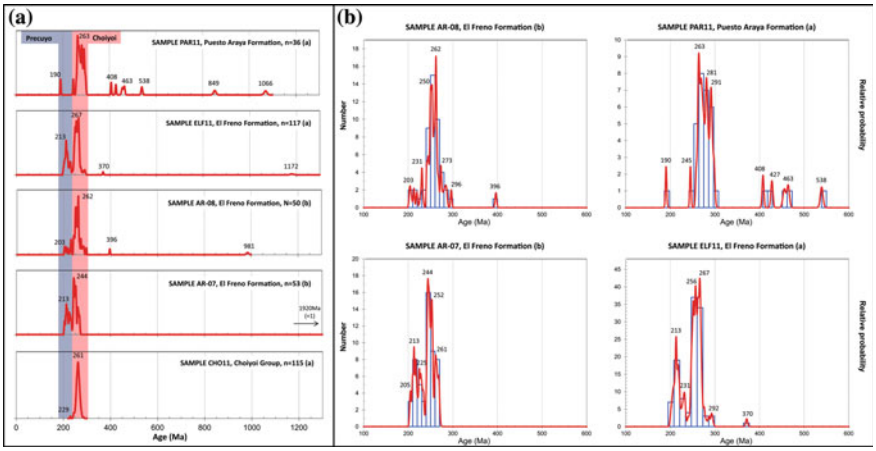

Fig. 3 **A** Probability density plots showing compiled U-Pb LA-ICP-MS geochronologic data, with shaded color bars highlighting major age populations and their probable source units. **B** Age histograms and probability density plots showing the main Phanerozoic peak ages for the El Freno and Puesto Araya Formations. Note that the samples from the older El Freno Formation contain principally 280–200 Ma grains, while the younger Puesto Araya Formation contains mostly 300–260 Ma grains, possibly reflecting progressive exhumation of older Choiyoi basement (Horton et al. 2016). This progressive exhumation is also supported by the higher abundance of older Paleozoic zircons in the Puesto Araya sample. Data obtained from (a) Horton et al. (2016), and (b) Naipauer et al. (2015)

of the Borbollón–La Manga lineament, all these mentioned units are absent at the base of the Mesozoic sedimentary pile, as borehole data evidence (Fig. 4; Bechis et al. 2010; Fuentes et al. 2016).

The Middle Jurassic to Paleogene infill of the Neuquén Basin in this sector consists of a thick succession of evaporitic, calcareous and clastic marine and continental

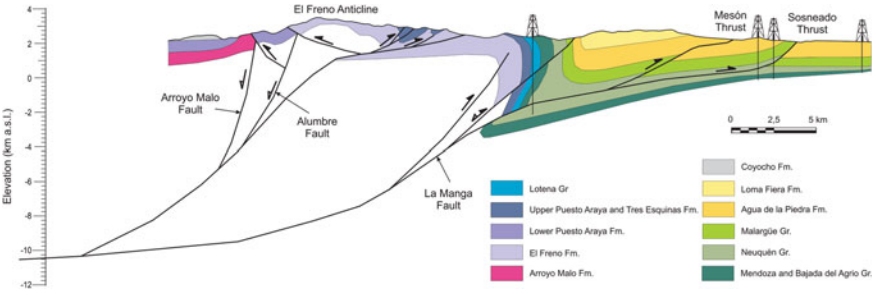

Fig. 4 Vertical cross section showing the present structural configuration of the fold and thrust belt in the Atuel depocenter area (modified from Giambiagi et al. 2012), where the main Mesozoic normal faults have been cut or inverted during the Andean shortening. Lateral thickness variations of the Late Triassic to Early Jurassic infill of the Atuel depocenter are also represented. See location on Fig. 2

sedimentary rocks, assigned to the upper Cuyo, Lotena, Mendoza, Bajada del Agrio, Neuquén, and Malargüe Groups (Fig. 2; Legarreta et al. 1993; Gulisano and Gutiérrez Pleimling 1994; Legarreta and Uliana 1996). The general thickness of this section increases toward the west, and proximal facies deposited at the basin margin crop out in the southern sector of the Frontal Cordillera, at the Cordón del Carrizalito range (Fig. 2).

Finally, the Cenozoic magmatic rocks are represented by Miocene to Quaternary andesitic to basaltic volcanic and subvolcanic rocks of the Molle, Huincán, Coyocho and Cerro Guanaquero Formations, and the Cerro Blanco Porphyry (Fig. 2; Volkheimer 1978; Baldauf 1997; Nullo et al. 2002; Sruoga et al. 2005; Giambiagi et al. 2008b). Thick clastic and volcaniclastic deposits of the Miocene to Holocene synorogenic infill of the Andean foreland basin crop out in the eastern sector, being represented by the Agua de la Piedra, Loma Fiera, Río Diamante, Mesones, La Invernada and Las Tunas Formations (Fig. 2; Yrigoyen 1993; Baldauf 1997; Combina and Nullo 2000; Giambiagi et al. 2008b; Horton et al. 2016).

4.1 Depocenter Infilling During the Late Triassic to Early Jurassic

The stratigraphic setting of the infill of the Atuel depocenter allows differentiating two contrasting areas interpreted as the Arroyo Malo half-graben to the west and the Río Blanco half-graben to the east (Fig. 5; Giambiagi et al. 2008a; Lanés 2005; Lanés et al. 2008).

In the western sector, in the Arroyo Malo half-graben, marine deposits of three coarsening- and thickening-upward cycles of mudstones, sandstones, and conglomerates assigned to the Arroyo Malo Formation and to the lower section of the Puesto Araya Formation, of Rhaetian to late Early Sinemurian age, crop out (Fig. 5; Riccardi et al. 1988, 1997; von Hillebrandt 1989; Riccardi and Iglesia Llanos 1999; Lanés, 2005; Lanés et al. 2008). These successions were interpreted as deposited in shallowing-upward, fluvio-dominated, transverse, normal-fault-controlled, slope-type fan deltas, with the uppermost section representing intermediate shelf to Gilbert-type fan deltas (Lanés 2005).

To the east, in the Rio Blanco half-graben, fining- to coarsening-upward and thinning-upward fluvial successions of lensoidal conglomerates, sandstones, and minor mudstones of the El Freno Formation appear (Fig. 5; Reijeinstein 1967; Artabe et al. 2005; Giambiagi et al. 2005a; Spalletti et al. 2007; Lanés et al. 2008). Interestingly, the geometry and connectivity of the fluvial channels changed along the time from wide ribbons at the base to isolated ribbons surrounded by fines in the middle section, to belts and eventually wider mobile-channel belts at the top (Lanés et al. 2008). These fluvial deposits are sharply overlain by well bedded, fining, and thinning-upward marine sandstones and shales that record a transgressive siliciclastic storm-dominated shelf, evolving from a wave-dominated estuary to a turbidite

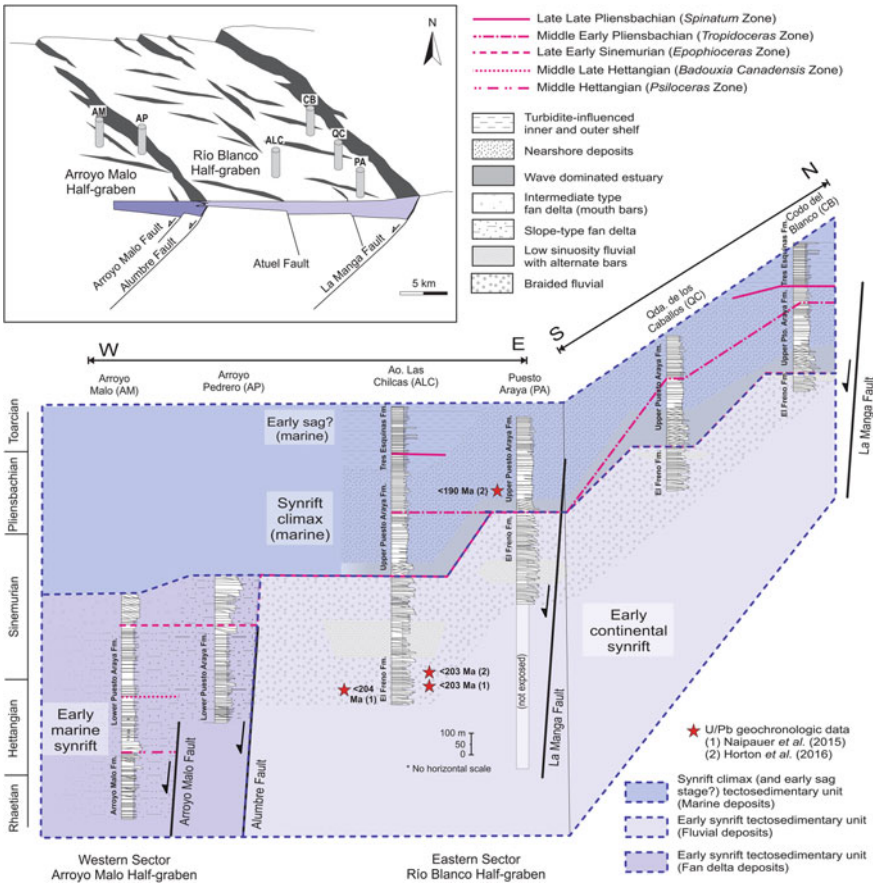

Fig. 5 Stratigraphic setting of the Atuel depocenter infill with biostratigraphic correlation of the vertical sections studied by Lanés (2005) and Lanés et al. (2008). Block diagram shows location of the vertical sections in relation with the main normal faults (modified from Giambiagi et al. 2008a)

outer shelf (Lanés 2005). The basal part of the marine deposits was assigned to the upper section of the Puesto Araya Formation (late Early Sinemurian to Toarcian), transitionally followed by the shales of the Tres Esquinas Formation (Late Pliensbachian–Bajocian), deposited in an anaerobic turbidite marine shelf (Fig. 5; Lanés 2005; Lanés et al. 2008).

The age and correlation of the marine units (Arroyo Malo, Puesto Araya, and Tres Esquinas Formations) were based on a detailed ammonite, bivalve, and brachiopod biostratigraphy (Fig. 5; Riccardi et al. 1991; Riccardi and Damborenea 1993; Lanés 2005; Lanés et al. 2008). Although the base of the Atuel depocenter infill is always below the present exposure level, biostratigraphic data from the outcropping deposits evidence a strong diachronicity for the start of marine sedimentation, varying from Late Triassic in the western sector, up to Early Pliensbachian at its southeastern

sector (Fig. 5; Lanés 2005; Lanés et al. 2008). A recent U-Pb (LA-ICP-MS) analysis from detrital zircons of the Puesto Araya Formation in the southeastern sector found a youngest age data of 190.5 ± 3.0 Ma, constraining the maximum sedimentation age at the Early Pliensbachian and confirming previous biostratigraphic data (Fig. 3; Horton et al. 2016). Conversely, age determination of the El Freno Formation was more problematic due to the lack of accurate biostratigraphic markers, though its paleofloristic content yielded a general Early Jurassic age (Herbst 1968; Artabe et al. 2005; Spalletti et al. 2007). Detrital zircons recently dated by U-Pb (LA-ICP-MS) gave youngest populations between 213 and 203 Ma, representing a Late Triassic maximum sedimentation age for the unit (Fig. 3; Naipauer et al. 2015; Horton et al. 2016). Considering that the age of the overlying marine deposits of the upper section of the Puesto Araya Formation varies between the late Early Sinemurian and the Early Pliensbachian (Fig. 5; Riccardi et al. 1991; Lanés 2005), the available biostratigraphic and geochronologic data constrain the age of the El Freno Formation between the late Rhaetian and the Early Pliensbachian. These data support the lateral correlation of the fluvial deposits with the fan-deltaic sequences of the lower section of the Puesto Araya Formation in the western area, proposed by previous stratigraphic, sedimentologic, structural and petrographic studies (Fig. 5; Lanés et al. 2008; Tunik et al. 2008; Giambiagi et al. 2008a).

4.2 Sedimentary Provenance Data

Sandstone petrographic characterization of the Atuel depocenter infill units allowed identifying four petrofacies (Tunik et al. 2008, 2011) using the discrimination diagrams of Dickinson et al. (1983; Fig. 6).

The Petrofacies A characterizes the Arroyo Malo Formation and indicates provenance from a transitional arc (Fig. 6; Tunik et al. 2008). It has low quartz and feldspars content and abundant lithic fragments mainly of felsic and mafic volcanic rocks and subordinated plutonic, sedimentary, and pyroclastic rocks fragments. The low mineralogical maturity of this petrofacies suggests short transport from source areas.

The Petrofacies B includes El Freno Formation and the lower section of Puesto Araya Formation, which show similar petrographic characteristics and provenance from a volcanic arc to a dissected arc (Fig. 6; Tunik et al. 2008). This petrofacies is characterized by a remarkable increase in the quartz and feldspar proportion and a lower lithic fragment content of mainly felsic volcanic rocks. The petrographic data support coetaneous sedimentation of the fluvial deposits of the El Freno Formation to the east and the fan-deltaic deposits of the lower section of the Puesto Araya Formation to the west, as previous studies proposed (Lanés et al. 2008; Giambiagi et al. 2008a).

The Petrofacies C, assigned to the upper Puesto Araya Formation, indicates a dissected arc to a recycled orogen provenance (Fig. 6; Tunik et al. 2008). It shows higher quartz content due to a noticeable increase in polycrystalline quartz and similar abundance of monocrystalline quartz, and subordinated feldspar and felsic lithic

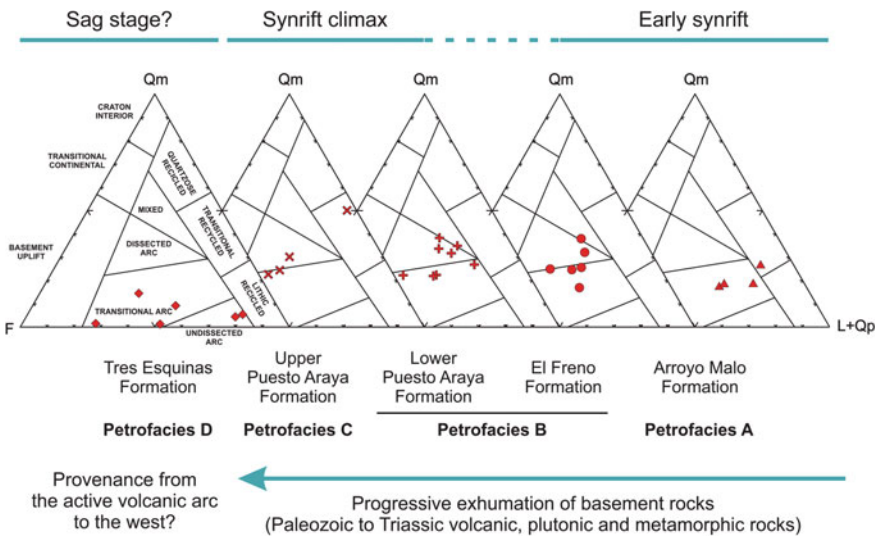

Fig. 6 Detrital sandstone mode for the four petrofacies recognized by Tunik et al. (2008, 2011), plotted in source discrimination diagrams (Dickinson et al. 1983). Qm: monocrystalline quartz, F: total feldspar, L + Qp: total lithics and polycrystalline quartz

fragments. Some of the quartz and feldspars grains show myrmekitic and graphic textures. Therefore, composition and textures point to felsic volcanic and plutonic sources.

Finally, the Petrofacies D is related to the Tres Esquinas Formation and equivalent units located to the west of the Atuel depocenter and revealed provenance from a transitional or undissected arc (Fig. 6; Tunik et al. 2011). This petrofacies composition is very different from the rest with very low quartz and variable feldspar content, with plagioclase more abundant than alkali feldspar. Lithic fragments show higher proportion of basic volcanic rocks respect to felsic textures, while plutonic and metamorphic clasts are uncommon. Volcanic shards found in the matrix and neovolcanic ignimbrites and devitrification lithic clasts indicate active volcanism during deposition of this petrofacies.

5 Structural Setting

In the Atuel depocenter, Mesozoic normal faults have been classified into four orders according to their dimensions and control over synrift subsidence (Bechis et al. 2010). The major normal faults have been inverted or cut by the Andean contractional structures or covered by younger deposits (Giambiagi et al. 2008b; Bechis et al. 2010; Fuentes et al. 2016). Therefore, three lines of evidence have been combined in order to identify the normal faults: (1) controls of the previous extensional structures

over the Andean shortening; (2) angular and progressive unconformities within the synrift units, indicating syntectonic sedimentation; and (3) lateral facies and thickness variations of the synrift deposits (Lanés, 2002, 2005; Lanés et al. 2008; Giambiagi et al. 2005a, 2008a; Bechis et al. 2009, 2010). These first- and second-order normal faults are shown in Fig. 7 and described in Sect. 5.1.

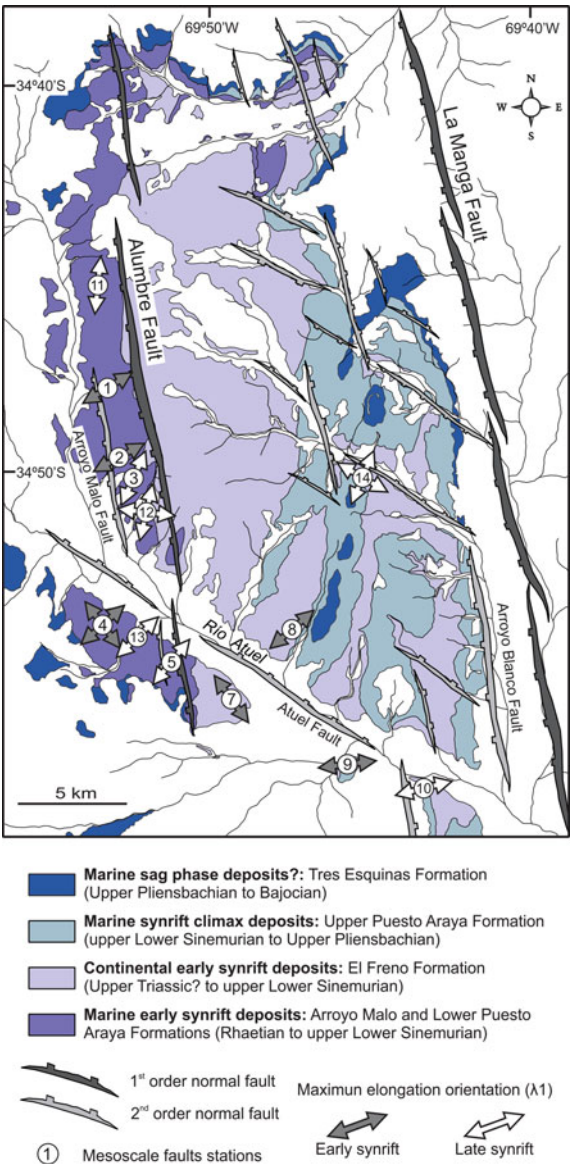

Fig. 7 Map showing the Late Triassic to Early Jurassic extensional architecture of the Atuel depocenter composed of first- and second-order normal faults interpreted by Lanés (2005), Lanés et al. (2008), Giambiagi et al. (2008a) and Bechis et al. (2010). Location of the mesoscale fault stations analyzed in Figs. 8 and 9 is also shown on the map, with double arrows indicating the orientation of the major axis of the obtained strain ellipsoids (λ1). Early synrift data correspond to faults affecting Upper Triassic to Hettangian deposits, while late synrift data were measured in Sinemurian to Pliensbachian deposits. See location of the map on Fig. 2

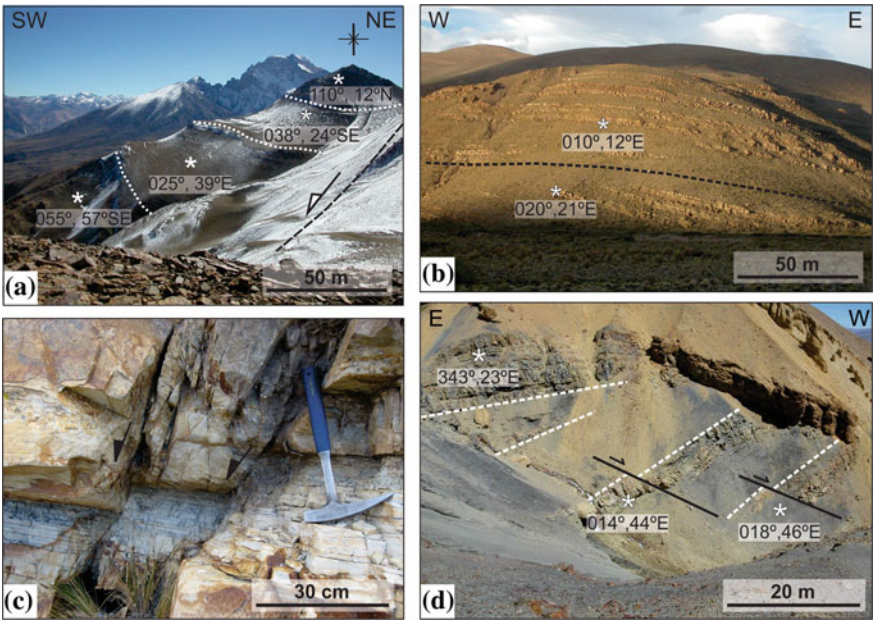

Fig. 8 **a** Syntectonic progressive unconconformities registered in the fan-deltaic synrift deposits of the hanging-wall of the Alumbre fault (from Giambiagi et al. 2008a). **b** Angular unconformity affecting the fluvial synrift deposits, in the hanging-wall of the La Manga fault (from Bechis et al. 2010). **c** Outcrop-scale faults registered in the southeastern sector of the Río Blanco half-graben (from Bechis et al. 2010). **d** Small-scale faults and related unconformities in the northern sector of the Arroyo Malo half-graben (from Bechis et al. 2010)

On the other hand, mesoscale faults with centimeter- to meter-scale displacements are generally well preserved, and more than 300 outcrop-scale normal faults affecting the synrift strata were recorded (Figs. 8, 9, and 10; Giambiagi et al. 2008a; Bechis et al. 2009, 2010). Field measurements of fault-slip data (fault orientation and direction and sense of slip from kinematic indicators) have been taken on these third and fourth scale faults, and kinematic analysis of these data from previous publications is included in Sect. 5.2 (Kinematic analysis, stations 1–12). Besides, we have also included new data to the kinematic analysis (stations 13 and 14) and we have carried out a new dynamic analysis of the data set, which is presented in Sect. 5.3.

5.1 Geometric Analysis

Two first-order, NNW-striking faults, the La Manga and Alumbre faults, controlled the orientation of the Atuel depocenter, as well as the distribution of sedimentary environments and drainage patterns (Figs. 5 and 7; Lanés 2002, 2005; Lanés et al. 2008; Giambiagi et al. 2008a). The La Manga fault was interpreted as the eastern

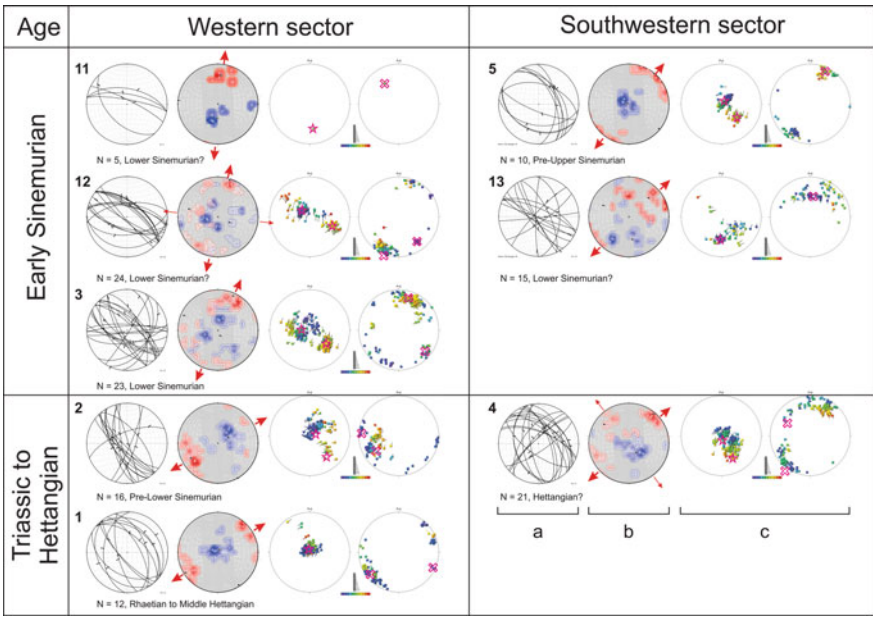

Fig. 9 Kinematic and dynamic analysis of mesoscale faults from the western sector of the Atuel depocenter. Location of measurement stations is shown on Fig. 7. **a** Major circles representing the lower-hemisphere projection of fault planes, with arrows showing the hanging-wall sense of movement. **b** Kinematic diagrams obtained with the FaultKinWin® software (Marrett and Allmendinger 1990; Allmendinger et al. 2012). Distribution of principal incremental shortening axes (*P* axes, blue dots) and extension axes (*T* axes, red dots) for each fault. Black squares represent the obtained axes of the strain ellipsoid ($\lambda 1$, $\lambda 2$ and $\lambda 3$) for every group of faults. Both *P*- and *T*-axis 1% area contours are also shown. Big and small red arrows show the main and secondary extension directions. **c** Diagrams showing the principal orientations of stress axes detected by the multiple inverse method (Yamaji 2000, 2003). The stereograms use lower-hemisphere, equal-area projection. Clusters of symbols with similar colors and similar attitudes on the stereograms represent significant stresses for each set of fault-slip data. Left and right diagrams show results for the maximum ($\sigma 1$) and minimum ($\sigma 3$) stress axes, respectively. Pink stars ($\sigma 1$) and crosses ($\sigma 3$) indicate clusters of the obtained stress axes. Colors indicate the obtained value for the stress ratio $\phi = (\sigma 2 - \sigma 3)/(\sigma 1 - \sigma 3)$. Blue colors for ϕ close to 0 and red for ϕ close to 1. Kinematic data taken from Bechis et al. (2010), except station 13. The number of field data (*N*) and the age of the strata where the faults were observed are also indicated in the figure

border of the depocenter, located along the Borbollón–La Manga lineament, and the Río Blanco half-graben was developed on its hanging-wall. To the east of La Manga fault, there is no record of Upper Triassic to Lower Jurassic synrift deposits neither in outcrops nor in wells, while more than 1500 m of continental synrift strata are recorded on its hanging-wall to the west (Fig. 4; Bechis et al. 2010). Angular unconformities and outcrop-scale normal faults registered on its hanging-wall suggest that this structure remained active until at least Early Pliensbachian times (Fig. 8; Bechis et al. 2010).

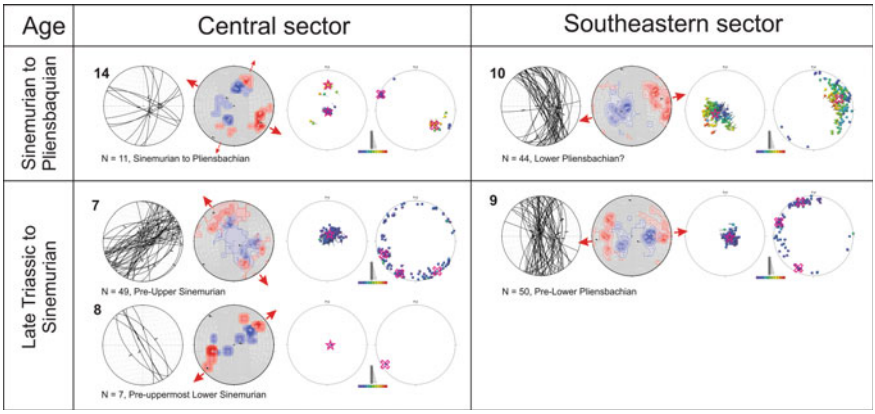

Fig. 10 Kinematic and dynamic analysis of mesoscale faults from the central and eastern sectors of the Atuel depocenter. Location of measurement stations is shown on Fig. 7. Diagram symbology is explained in Fig. 9 caption. Kinematic data taken from Bechis et al. (2010), except station 14

The Alumbre fault was proposed by Lanés et al. (2008) and Giambiagi et al. (2008a) as a WSW-dipping normal fault controlling the coastal line from middle Hettangian to Early Sinemurian times (Figs. 5 and 7). To the west of this fault, the fan-delta deposits of the synrift infill of the Arroyo Alumbre half-graben show a marked wedge geometry, with strata thickening toward the fault and syntectonic angular and progressive unconformities (Fig. 8; Giambiagi et al. 2008a; Bechis et al. 2010). A decrease in the accommodation in the uppermost fan-deltaic deposits on its hanging-wall suggests deactivation of the Alumbre fault by the late Early Sinemurian (Lanés 2005; Lanés et al. 2008).

Second-order faults show a bimodal distribution of NNW and WNW strikes (Fig. 7; Giambiagi et al. 2008a; Bechis et al. 2009, 2010). These structures are associated with synsedimentary deformation, such as abundant slumps within the slope-type fan-deltaic deposits (Lanés 2002), and angular and progressive unconformities within the continental and marine deposits (Bechis et al. 2010). The Arroyo Malo fault, synthetic to the Alumbre fault, was only active during the early synrift stage from the Late Triassic until the middle Hettangian, as sedimentary reactivations observed in the Arroyo Malo section evidence (Figs. 5 and 7; Lanés 2005; Lanés et al. 2008). The Atuel fault is a WNW-striking, inferred structure, which controlled variations in the depth of the fan-deltaic environment in the Arroyo Malo half-graben, with relatively higher depths registered on its hanging-wall to the north (Giambiagi et al. 2008a).

Outcrop-scale third- to fourth-order faults show variable orientation with most faults strikes ranging between NNW and NW, and secondary NNE, NE, and ENE fault populations (Giambiagi et al. 2005a; Bechis et al. 2010).

5.2 Kinematic Analysis

This section presents results from the kinematic analysis carried out by Bechis et al. (2010), together with new data. This analysis consists in obtaining the principal axes of the strain ellipsoid for outcrop-scale faults. Shortening and extension axes and moment tensor solutions were obtained for the different fault populations using the FaultKinWin® software (Marrett and Allmendinger 1990; Allmendinger et al. 2012). The results are shown in Figs. 7, 9 and 10. Data were collected along four sectors within the Atuel depocenter: western (stations 1, 2, 3, 11, and 12), southwestern (stations 4, 5, and 13), southeastern (stations 9 and 10), and central (stations 7, 8 and 14). All data were unfolded to their original position previous to the Andean contractional deformation. The obtained intermediate and major principal axes of the strain ellipsoid ($\lambda 2$ and $\lambda 1$) generally show a subhorizontal position, indicating an extensional tectonic regime, with a subvertical minimum principal axis ($\lambda 3$).

All along and across the studied depocenter, kinematic data indicate a main extensional direction ($\lambda 1$) with a NE to NNE orientation and a secondary extensional direction with a NW to WNW orientation (Figs. 9 and 10). Kinematic data from the western sector indicate a NE extensional direction for the Triassic to Hettangian period and a NNE extensional direction for the Sinemurian period (Fig. 9). Data from the southwestern and central sectors show two clusters of extensional axes, one indicating a principal NE extensional direction and the other one a NW extensional direction (Figs. 9 and 10). A large and representative dataset from station 7, located in the south-central sector, suggests a NW extensional direction. Data from the southeastern sector, close to the La Manga normal fault (stations 9 and 10), show a clear ENE extensional direction, perpendicular to this master fault (Fig. 10).

5.3 Dynamic Analysis

The dynamic analysis consists on paleostress computation from the fault-slip data to obtain the reduced stress tensor, which describes the shape of the stress ellipsoid (orientation of the principal stress axes and the ratio of the principal stress differences $\phi = (\sigma 2 - \sigma 3)/(\sigma 1 - \sigma 3)$). For this analysis, we used the Multiple Inverse Method proposed by Yamaji (2000), which allows the identification of different stress tensors from an heterogeneous fault-slip dataset. We obtained 25 well-constrained reduced paleostress tensor solutions for the Triassic-Hettangian, Sinemurian, and Pliensbachian periods. The results are presented as paired stereoplots showing the orientation of $\sigma 1$ (stars) and $\sigma 3$ (crosses), respectively (Figs. 9 and 10). In all tensors except tensor 13, $\sigma 1$ has a subvertical orientation with a distinctive cluster, and $\sigma 3$ and $\sigma 2$ are subhorizontal, indicating an extensional stress field, in agreement with the orientation of the kinematic axes. Some stations show an azimuthal dispersion of $\sigma 3$ (stations 2, 7, 9, 10, and 13), and others show two or more clusters of $\sigma 3$ (stations 1, 3, and 14).

Most of the tensors have low values of stress ratio ϕ (blue and violet colors in Figs. 9 and 10), suggesting that $\sigma 3$ and $\sigma 2$ are similar in magnitude. Despite that, other tensors (stations 3, 4, 5, 12) show high values of ϕ (orange and red colors) indicating magnitudes of $\sigma 2$ closer to $\sigma 1$ than to $\sigma 3$, which can be interpreted as an extensional/strike-slip regime. The high consistency and wide distribution of the extensional stress states with NNE- to ENE- and NW-oriented $\sigma 3$ and general low values of ϕ indicate that these stress configurations are related to a stress field controlling deformation locally inside the Atuel depocenter.

6 Discussion

6.1 Tectonic Implications for the Kinematic and Dynamic Analyses

Taking into account the orientation and shape of the strain and stress tensors, their distribution and timing, and the relationship between strain and stress axes, we constructed a dynamic model to explain the generation/reactivation of structures, their kinematics, and their evolution through time. Variations between the principal strain and stress axes may indicate that assumptions made for the paleostress analysis are not necessarily satisfied (Kaven et al. 2011). The critical analysis of these variations may shed light into additional assumptions that are required to interpret the stress regimes. Some of these assumptions are (i) mechanically anisotropic material (Jaeger et al. 2007; Hu and Angelier 2004), (ii) preexisting plane of weakness (Marrett and Allmendinger 1990; Nieto-Samaniego 1999; Martinez Días 2002), or (iii) rotations of blocks bounded by major faults (Twiss and Unruh 1998). Clusters of $\sigma 3$ obtained from the dynamic analysis correlate well with the extensional axes obtained from the kinematic analysis (stations 1, 3, 4, 5, 8, 12, and 14), while those stress tensors with a girdle distribution of $\sigma 3$ (stations 2, 7, 9, 10, and 13) differ from the results of the kinematic analysis (Figs. 9 and 10).

During the Late Triassic–late Hettangian period, extensional directions were slightly oblique to the Alumbre fault, in the Arroyo Malo half-graben (stations 1, 2, and 4; Figs. 7, 9 and 11) and perpendicular to the La Manga fault, in the eastern border of the Río Blanco half-graben (station 9; Figs. 7, 10 and 11). The stress ratio values of these tensors indicate close values of $\sigma 3$ and $\sigma 2$. Tensor 4 shows two-orthogonal clusters of $\sigma 3$ (Figs. 9 and 11), which together with low values of stress ratios suggest a $\sigma 2/\sigma 3$ permutation. Inside the Río Blanco half-graben, the kinematic analysis shows that extension was bimodal, with NW and NE directions (stations 7 and 8; Figs. 10 and 11). The NW direction was previously interpreted as probably related to local extension in the hinge zone of Andean anticlines (Bechis et al. 2010). However, the paleostress analysis suggests that the bimodal pattern responds to a local permutation of $\sigma 2$ and $\sigma 3$ during the Mesozoic synrift, in agreement with the values obtained from the stations close to the Alumbre and La Manga faults. We

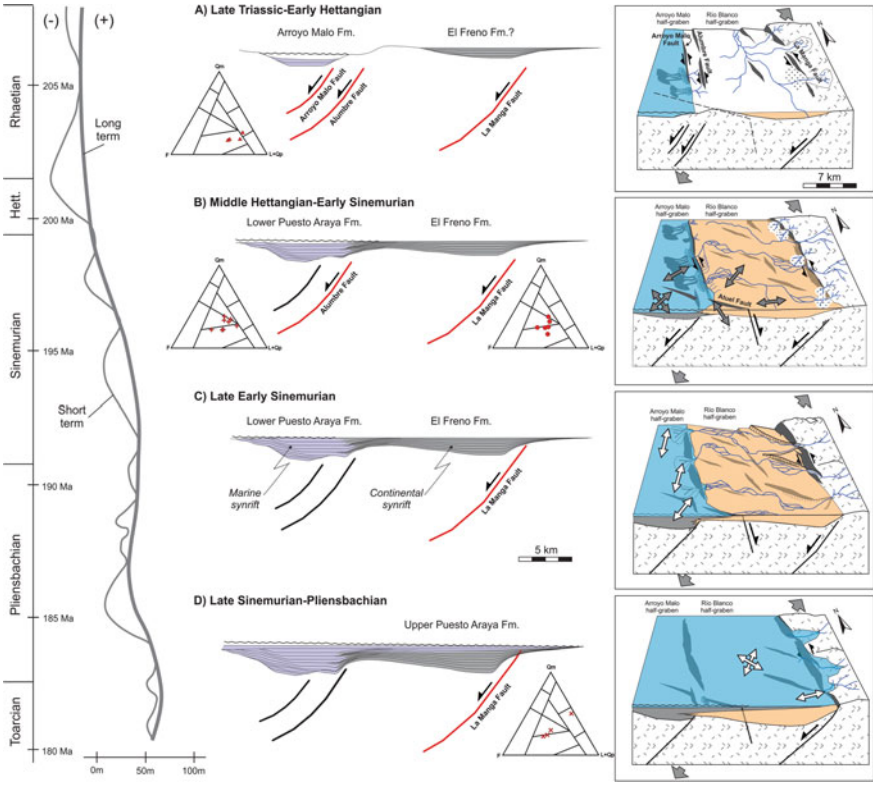

Fig. 11 2D and 3D diagrams showing the main stages of the interpreted tectono-stratigraphic evolution of the Atuel depocenter during the synrift stage (Late Triassic–Pliensbachian). Red colors highlight faults that were active at each stage. Thick gray arrows indicate the interpreted regional direction of extension, while double gray (early synrift) and white (late synrift) arrows show local variations in the extension inside the depocenter. Simplified diagrams showing petrographic provenance data for each unit were also included. The long- and short-term variations of the global eustatic level proposed by Haq et al. (1987) are also shown

interpret that, during the first stage of extension, deformation was focussed on pre-existing NNW-striking faults, such as the La Manga and Alumbre faults. Extensional movement along these structures might have perturbated the local stress field, with magnitudes of $\sigma 2$ close to $\sigma 3$, and local $\sigma 2/\sigma 3$ stress permutations.

During the Sinemurian to Pliensbachian period, the Arroyo Malo half-graben experienced a pure extension with NNE-oriented $\sigma 3$ (stations 3, 11, and 12; Figs. 7 and 9), in concomitance with a progressive deactivation of the Alumbre fault (Fig. 11). This extensional direction is interpreted as reflecting the regional stress regime, in agreement with previous proposals for the regional extension based on kinematic data (Bechis et al. 2010, 2014). On the contrary, in the Río Blanco half-graben, extensional directions are either NW- and NNE-oriented in the central sector (station 14; Figs. 7, 10 and 11) or ENE-oriented near La Manga fault (station 10; Figs. 7, 10

and 11). This is interpreted here as reflecting a strain partitioning between a NNE extension, subparallel to the regional extension direction, and an ENE extension orthogonal to the NNW-striking preexisting La Manga fault.

Our results are consistent with previous kinematic analysis where the Atuel depocenter was interpreted to have been formed by oblique reactivation of NNW-striking anisotropies under a regional NNE extension (Giambiagi et al. 2008a; Bechis et al. 2009, 2010, 2014). The high obliquity between the NNW orientation of the rift system, controlled by the first-order normal faults, and the NNE regional extension would result in a wrench dominated transtension (Tikoff and Teyssier 1994; Teyssier et al. 1995; De Paola et al. 2005; Bechis et al. 2014). This type of transtensional strain produces a complex structural pattern of normal, oblique, and strike-slip faults. Deformation could be either distributed or partitioned, and switching of the main axis of the strain ellipsoid may occur along the evolution of the system, due to finite strain localized along major faults. The results of our kinematic and dynamic analyses show a complex distribution and evolution of the strain and stress inside the Atuel depocenter, which is consistent with predictions from analytical and experimental models of highly oblique rift systems (Tikoff and Teyssier 1994; Bechis et al. 2014). The obtained results suggesting bimodal and/or radial horizontal extension, together with reactivation of NNW-striking anisotropies, also explain the variation in strike of the master faults of the nearby depocenters, between the NNW-trending Atuel, Malargüe and Palauco, and the NNE- to NE-trending Río del Cobre and Valenciana depocenters (Fig. 1).

We infer an important strain localization in the Alumbre and La Manga faults that was responsible for several particular characteristics of the Atuel and Malargüe depocenters, such as: (i) the marked NNW orientation of the depocenters, controlled by the La Manga and Malargüe faults, respectively, (ii) the early marine transgression localized in the hanging-wall of the Alumbre fault, with the only Triassic to Hettangian marine deposits of the entire Neuquén Basin, and (iii) the particular distribution of depositional environments until the end of the Early Sinemurian, as the Alumbre fault limited the marine transgression to the western sector of the depocenter, while the La Manga fault controlled the fluvial sedimentation in the eastern sector.

6.2 Tectono-Stratigraphic Evolution

We integrated the available structural, sedimentologic, petrographic, and geochronologic data into a tectono-stratigraphic model for the evolution of the Atuel depocenter (Fig. 11), whose extensional phase prevailed at least from Rhaetian to Pliensbachian times. A complex interplay between tectonic subsidence related to the activity of the major normal faults and eustatic sea-level changes controlled the evolution of this sector of the Neuquén Basin during the synrift stage.

We interpret the Rhaetian to early Hettangian sediments as deposited during the early synrift phase of the Atuel depocenter, when a paleogeography dominated by early formed fault segments controlled the marked variations in sedimentary fill

(Stage A; Fig. 11). Provenance analysis of the fan-deltaic deposits indicates short transport from local source areas (Tunik et al. 2008), suggesting that the Arroyo Malo and Río Blanco half-grabens were isolated at that time.

During the middle Hettangian to Early Sinemurian (Stage B; Fig. 11), some former fault segments became inactive (i.e., Arroyo Malo fault; Lanés et al. 2008), while other faults gained length and displacement, probably due to the connection of different fault segments (i.e., Alumbre and La Manga faults). The Alumbre fault maintained a nearly fixed position of the coastal line, restricting the marine sedimentation to the western sector of the depocenter. While a braided fluvial system characterizes the synrift infill in the hanging-wall of the La Manga fault during this stage, coetaneous deposits to the west of the Alumbre fault were deposited in a slope-type fan-deltaic environment (Lanés 2002, 2005; Lanés et al. 2008; Tunik et al. 2008).

During the late Early Sinemurian (Stage C; Fig. 11), an eustatic short-term lowstand (Haq et al. 1987) led to fluvial incision on the shelf and fan-deltaic conglomerate deposition in the Arroyo Malo half-graben (Lanés et al. 2008). A subsequent slow sea-level rise increased the accommodation on the hanging-wall of the Alumbre fault, allowing the fan-deltaic mouth bars to prograde (Lanés 2005; Lanés et al. 2008). The restricted accommodation needed for the progradation of the intermediate fan-delta mouth bars suggests deactivation of the Alumbre fault by this stage.

Thereafter, a faster sea-level rise and an important increase of accommodation allowed estuarine deposition in the Río Blanco half-graben (Lanés 2005; Lanés et al. 2008). The decreasing accommodation observed by the end of the Early Sinemurian in the Arroyo Malo half-graben was previously related to the start of the sag phase (Lanés 2005; Lanés et al. 2008). However, the subsequent creation of accommodation in the Río Blanco half-graben, together with the observed outcrop-scale faults affecting Pliensbachian sediments in the southeastern sector of the depocenter (station 10; Fig. 10), suggest that the extensional deformation continued up to this time. We interpret the Late Sinemurian–Pliensbachian (Stage D; Fig. 11) as a period of rift climax associated with important movement along the La Manga master fault (through-going fault zone stage; Gawthorpe and Leeder 2000). During this climax phase, the marine coastal line was controlled by the La Manga and Valenciana master faults.

Provenance data suggest an important basin reorganization by the Toarcian (Tunik et al. 2008, 2011). Petrographic and geochronologic data from Arroyo Malo, El Freno, and Puesto Araya Formations suggest progressive exhumation of the Permo-Triassic magmatic belt during the Hettangian to Pliensbachian period (Figs. 3 and 6; Tunik et al. 2008, 2011; Naipauer et al. 2015; Horton et al. 2016), probably due to normal fault activity. On the contrary, petrographic data of the latest Pliensbachian to Bajocian Tres Esquinas Formation indicate a major change in the source area, as is evidenced by the low quartz content, while a contemporaneous volcanic source, probably located to the west of the basin, was incorporated. This change could be related to the deactivation of the La Manga fault and the initiation of the sag stage in the Atuel depocenter.

7 Concluding Remarks

We compiled, analyzed, and integrated a large set of the previous sedimentologic, petrographic, geochronologic, and structural data from the Atuel depocenter. Geometrical, kinematic and dynamic analysis of structural data allowed us to construct a model explaining the generation and reactivation of structures, their kinematics, and their evolution through time. Reactivation of preexisting NNW-striking anisotropies under a regional NNE extension resulted in an oblique rift setting, which generated a bimodal distribution of NNW- and WNW-striking major normal faults. Concentration of deformation along reactivated NNW-striking faults generated a local stress field superposed to a regional NNE regional extension leading to an in situ stress field with values of $\sigma 2$ close to $\sigma 3$ and local $\sigma 2/\sigma 3$ stress permutations. Contemporaneous NNE- and ENE-oriented extensional directions are probably related to strain partitioning between a NNE extension, subparallel to the regional extension direction, and an ENE extension orthogonal to the NNW-striking preexisting major faults.

Sedimentologic and petrographic data revealed a complex evolution with strong lateral variations of the depositional environments during the synrift stage, mainly controlled by tectonic subsidence related to the activity of the major normal faults and eustatic sea-level changes. The NNW-striking La Manga and Alumbre master faults controlled most of the basin subsidence, the distribution of the sedimentary environments, and the drainage patterns. The Arroyo Malo half-graben developed on the hanging-wall of the Alumbre fault, in the western sector of the depocenter, and beared an early marine synrift infill consisting of fan-deltaic deposits. Eastwards, the La Manga fault controlled subsidence in the Rio Blanco half-graben, whose synrift infill consists of fluvial deposits followed by marine beds deposited in a transgressive siliciclastic storm-dominated shelf.

We identified several stages for the evolution of the Atuel depocenter during the synrift phase, which took place from Rhaetian to Pliensbachian times. These stages were controlled by processes of initiation, propagation, growth, linkage, and deactivation of new and reactivated faults along the depocenter evolution, in combination with eustatic sea-level changes. Provenance data suggest an important basin reorganization by the Toarcian, which could be related to initiation of the sag stage in this depocenter.

Acknowledgements This research was funded by Agencia Nacional de Promoción Científica y Tecnológica (PICT 07-10942, PICT 38295, PICT-2015-1181), Consejo Nacional de Investigaciones Científicas y Técnicas (CONICET PIP 5843), and Universidad de Buenos Aires (UBACYT 855). We wish to give special thanks to Alejandro Celli, Gabriela Da Poian, Victor García, Diego Iaffa, Diego Kietzmann, Darío Orts, Sergio Orts, Marilin Peñalva, Carla Terrizzano, and Daniel Yagupsky for their invaluable help in the field and discussions. We thank Drs. Susana Damborenea, Miguel Manceñido, and Alberto Riccardi, for their comments about the biostratigraphic data. The subsurface information was kindly facilitated by Julián Fantín, Gonzalo Zamora Valcarce, Roberto Varade, and Tomás Zapata, from Repsol-YPF. We also thank Ernesto Cristallini for many fruitful discussions about the topic.

References

Allmendinger RW, Cardozo N, Fisher D (2012) Structural geology algorithms: vectors and tensors in structural geology. Cambridge University Press, Cambridge

Alvarez P, Ramos VA (1999) The Mercedario rift system in the principal Cordillera of Argentina and Chile (32° SL). J S Am Earth Sci 12:17–31

Artabe AE, Morel EM, Spalletti L et al (1998) Paleoambientes sedimentarios y paleoflora asociada en el Triásico tardío de Malargüe, Mendoza. Rev Asoc Geol Argent 53:526–584

Artabe AE, Ganuza DG, Spalletti LA et al (2005) Revisión de la paleoflora del cerro La Brea (Jurásico Temprano), provincia de Mendoza, Argentina. Ameghiniana 42:429–442

Astini RA, Benedetto JL, Vaccari NE (1995) The early Paleozoic evolution of the Argentine Precordillera as a Laurentian rifted, drifted, and collided terrane: A geodynamic model. Geol Soc Am Bull 107:253–273

Azcuy CL, Caminos R (1987) Diastrofismo. In: Archangelsky S (ed) El Sistema Carbonífero en la República Argentina. Academia Nacional de Ciencias, Córdoba, pp 239–251

Baldauf P (1997) Timing of the uplift of the Cordillera Principal, Mendoza Province, Argentina. Master thesis, George Washington University

Balgord EA, Carrapa B (2016) Basin evolution of Upper Cretaceous-Lower Cenozoic strata in the Malargüe fold and thrust belt: northern Neuquén Basin, Argentina. Basin Res 28:183–206

Barrionuevo M, Mescua JF, Giambiagi L et al (2019) Miocene deformation in the orogenic front of the Malargüe fold-and-thrust belt (35°30′–36° S): controls on the migration of magmatic and hydrocarbon fluids. Tectonophysics 766:480–499

Bechis F (2009) Deformación transtensiva de la cuenca Neuquina: análisis a partir de ejemplos de campo y modelos análogos. Ph.D. thesis, Universidad de Buenos Aires

Bechis F, Giambiagi LB, Lanés S et al (2009) Evidencias de extensión oblicua en los depósitos de sinrift del sector norte de la cuenca Neuquina. Rev Asoc Geol Argent 65:293–310

Bechis F, Giambiagi L, García V et al (2010) Kinematic analysis of a transtensional fault system: the Atuel depocenter of the Neuquén basin, southern Central Andes, Argentina. J Struct Geol 32:886–899

Bechis F, Cristallini E, Giambiagi L et al (2014) Transtensional tectonics induced by oblique reactivation of previous lithospheric anisotropies during the Late Triassic to Early Jurassic rifting in the Neuquén basin: insights from analog models. J Geodyn 79:1–17

Buchanan AS, Kietzmann DA, Palma RM (2017) Evolución paleoambiental de la Formación Remoredo (Jurásico inferior) en el depocentro Malargüe, Cuenca Neuquina Surmendocina. Rev Asoc Geol Argent 74:163–178

Carbone O, Franzese J, Limeres M et al (2011) El Ciclo Precuyano (Triásico Tardío-Jurásico Temprano) en la Cuenca Neuquina. In: Leanza HA, Arregui C, Carbone O et al (eds) Geología y Recursos Naturales de la Provincia del Neuquén. Asociación Geológica Argentina, Buenos Aires, pp 63–75

Charrier R (1979) El Triásico en Chile y regiones adyacentes de Argentina: Una reconstrucción paleogeográfica y paleoclimática. Departamento de Geología, Universidad de Chile, Santiago, Comunicaciones 26:1–47

Charrier R, Pinto L, Rodríguez MP (2007) Tectonostratigraphic evolution of the Andean Orogen in Chile. In: Moreno T, Gibbons W (eds) The geology of Chile. The Geological Society, London, pp 21–114

Cobbold PR, Rossello EA (2003) Aptian to recent compressional deformation, foothills of the Neuquén basin Argentina. Mar Petrol Geol 20:429–443

Combina AM, Nullo F (2000) La Formación Loma Fiera (Mioceno superior) y su relación con el volcanismo y el tectonismo neógeno, Mendoza. Rev Asoc Geol Argent 55:201–210

Cristallini EO, Tomezzoli RN, Pando G (2009) Controles precuyanos en la estructura de la cuenca Neuquina. Rev Asoc Geol Argent 65:248–264

Damborenea SE (1987) Early Jurassic bivalvia of Argentina. Part 1: Stratigraphical introduction and Superfamilies Nuculanacea, Arcacea, Mytilacea and Pinnacea. Palaeontogr A 199:23–111

Davidson J (1988) El Jurásico y Cretácico inferior en las nacientes del río Teno (Chile): una revisión. In: Abstracts of the 5° Congreso Geológico Chileno, Santiango de Chile, 8–12 Aug 1988
De Paola N, Holdsworth RE, McCaffrey KJ et al (2005) Partitioned transtension: an alternative to basin inversion models. J Struct Geol 27:607–625
Dicarlo DJ, Cristallini E (2007) Estructura de la margen norte del Río Grande, Bardas Blancas, provincia de Mendoza. Rev Asoc Geol Argentina 62:187–199
Dickinson WR, Beard LS, Brakenridge GR et al (1983) Provenance of North American Phanerozoic sandstones in relation to tectonic setting. Geol Soc Am Bull 94:222–235
Espinoza M, Montecino D, Oliveros V et al (2018) The synrift phase of the early Domeyko Basin (Triassic, northern Chile): sedimentary, volcanic and tectonic interplay in the evolution of an ancient subduction-related rift basin. Basin Res. https://doi.org/10.1111/bre.12305
Fennell LM, Folguera A, Naipauer M et al (2017) Cretaceous deformation of the southern Central Andes: synorogenic growth strata in the Neuquén Group (35° 30′–37° S). Basin Res 29:51–72
Franzese JR, Spalletti LA (2001) Late Triassic–early Jurassic continental extension in southwestern Gondwana: tectonic segmentation and pre-break-up rifting. J S Am Earth Sci 14:257–270
Fuentes F, Horton BK, Starck D et al (2016) Structure and tectonic evolution of hybrid thick-and thin-skinned systems in the Malargüe fold–thrust belt, Neuquén basin, Argentina. Geol Mag 153:1066–1084
García Morabito E, Ramos VA (2012) Andean evolution of the Aluminé fold and thrust belt, Northern Patagonian Andes (38° 30′–40°30′ S). J S Am Earth Sci 38:13–30
Gawthorpe RL, Leeder MR (2000) Tectono-sedimentary evolution of active extensional basins. Basin Res 12:195–218
Gerth E (1925) Estratigrafía y distribución de los sedimentos mesozoicos en los Andes Argentinos. Academia Nacional de Ciencias, vol 9, Cordoba, pp 11–55
Giambiagi LB, Martínez A (2008) Permo-Triassic oblique extension in the Potrerillos-Uspallata area, western Argentina. J S Am Earth Sci 26:252–260
Giambiagi LB, Alvarez P, Godoy E et al (2003a) The control of pre-existing extensional structures on the evolution of the southern sector of the Aconcagua fold and thrust belt, southern Andes. Tectonophysics 369:1–19
Giambiagi LB, Ramos VA, Godoy E et al (2003b) Cenozoic deformation and tectonic style of the Andes, between 33° and 34°. South Latitude. Tectonics 22:1041
Giambiagi LB, Suriano J, Mescua J (2005a) Extensión multiepisódica durante el Jurásico Temprano en el depocentro Atuel de la cuenca Neuquina. Rev Asoc Geol Argent 60:524–534
Giambiagi LB, Álvarez PP, Bechis F et al (2005b) Influencia de las estructuras de rift triásicas – jurásicas sobre el estilo de deformación en las fajas plegadas y corridas Aconcagua y Malargüe. Rev Asoc Geol Argent 60:661–671
Giambiagi LB, Bechis F, Lanés S et al (2008a) Formación y evolución triásico-jurásica del depocentro Atuel, cuenca Neuquina, provincia de Mendoza, Argentina. Rev Asoc Geol Argent 63:520–533
Giambiagi LB, Bechis F, García VH et al (2008b) Temporal and spatial relationships of thick-and thin-skinned deformation in the Malargüe fold and thrust belt, Southern Central Andes. Tectonophysics 459:123–139
Giambiagi LB, Tunik MA, Barredo S et al (2009a) Cinemática de apertura del sector norte de la cuenca Neuquina. Rev Asoc Geol Argent 65:278–292
Giambiagi LB, Ghiglione M, Cristallini E et al (2009b) Kinematic models of basement/cover interactions: insights from the Malargüe fold and thrust belt, Mendoza, Argentina. J Struct Geol 31:1443–1457
Giambiagi LB, Mescua JF, Bechis F et al (2011) Pre-Andean deformation of the Precordillera southern sector, southern Central Andes. Geosphere 7:219–239
Giambiagi LB, Mescua JF, Bechis F et al (2012) Thrust belts of the southern Central Andes: along-strike variations in shortening, topography, crustal geometry, and denudation. Geol Soc Am Bull 124:1339–1351

Giambiagi LB, Tassara A, Mescua JF et al (2014) Evolution of shallow and deep structures along the Maipo-Tunuyán transect (33° 40′ S): from the Pacific coast to the Andean foreland. In: Sepúlveda SA, Giambiagi LB, Moreiras S et al (eds) Geodynamic processes in the Andes of Central Chile and Argentina, The Geological Society, London, SP 399, p 63

Gómez R, Lothari L, Tunik MA et al (2019) Onset of foreland basin deposition in the Neuquén Basin (34°–35°S): new data from sedimentary petrology and U-Pb dating of detrital zircons from the Upper Cretaceous non-marine deposits. J S Am Earth Sci 95:102257

Gulisano CA (1981) El Ciclo Cuyano en el norte de Neuquén y sur de Mendoza. In: Abstracts of the 8 Congreso Geológico Argentino, San Luis, 20–26 Sept 1981

Gulisano CA, Gutiérrez Pleimling AR (1994) The Jurassic of the Neuquén Basin: b) Mendoza Province. Guía de Campo. Asociación Geológica Argentina, Buenos Aires, vol E3, pp 1–103

Haq BU, Hardenbol J, Vail PR (1987) Chronology of fluctuating sea levels since the Triassic. Science 235:1156–1167

Herbst R (1968) Las floras liásicas argentinas con consideraciones estratigráficas. In: Abstracts of the 3º Jornadas Geológicas Argentinas, Buenos Aires, pp 145–162

Horton BK, Fuentes F, Boll A et al (2016) Andean stratigraphic record of the transition from backarc extension to orogenic shortening: a case study from the northern Neuquén basin, Argentina. J S Am Earth Sci 71:17–40

Howell JA, Schwarz E, Spalletti LA et al (2005) The Neuquén Basin: an overview. In: Veiga GD, Spalletti LA, Howell JA et al (eds) The Neuquén Basin: a case study in sequence stratigraphy and basin dynamics. The Geological Society, London, SP 252, 1–14

Hu JC, Angelier J (2004) Stress permutations: three-dimensional distinct element analysis accounts for a common phenomenon in brittle tectonics. J Geoph Res 109:B09403

Jaeger JC, Cook NG, Zimmerman R (2007) Fundamentals of rock mechanics, 4th edn. Wiley-Blackwell, Oxford, p 488

Japas MS, Cortés JM, Pasini M (2008) Tectónica extensional triásica en el sector norte de la cuenca Cuyana: primeros datos cinemáticos. Rev Asoc Geol Argentina 63:213–222

Kaven JO, Maerten F, Pollard DD (2011) Mechanical analysis of fault slip data: Implications for paleostress analysis. J Struct Geol 33:78–91

Keidel J (1916) La geología de las sierras de la provincia de Buenos Aires y sus relaciones con las montañas del Cabo y los Andes. Ministerio de Agricultura de la Nación, Anales Dirección de Geología, Mineralogía y Minería 9:5–77

Kleiman LE, Japas MS (2009) The Choiyoi volcanic province at 34° S–36° S (San Rafael, Mendoza, Argentina): implications for the Late Palaeozoic evolution of the southwestern margin of Gondwana. Tectonophysics 473:283–299

Kokogian DA, Fernández Seveso F, Mosquera A (1993) Las secuencias sedimentarias Triásicas. In: Ramos VA (ed) Geología y recursos naturales de Mendoza. Asociación Geológica Argentina, Buenos Aires, pp 65–78

Kozlowski E, Manceda R, Ramos VA (1993) Estructura. In: Ramos VA (ed) Geología y recursos naturales de Mendoza. Asociación Geológica Argentina, Buenos Aires, pp 235–256

Lanés S (2002) Paleoambientes y Paleogeografía de la primera transgresión en Cuenca Neuquina, Sur de Mendoza. Ph.D. thesis, Universidad de Buenos Aires

Lanés S (2005) Late Triassic to Early Jurassic sedimentation in northern Neuquén Basin, Argentina: tectonosedimentary evolution of the first transgression. Geol Acta 3:81–106

Lanés S, Palma RM (1998) Environmental implications of oncoids and associated sediments from the Remoredo Formation (Lower Jurassic) Mendoza, Argentina. Palaeo 140:357–366

Lanés S, Salani FM (1998) Petrografía, origen y paleoambiente sedimentario de las piroclastitas de la Formación Remoredo (Jurásico Temprano), Argentina (35° 30′ S–70° 15′ W). Rev Geol Chile 25:141–152

Lanés S, Giambiagi LB, Bechis F et al (2008) Late Triassic—early Jurassic successions of the Atuel depocenter: sequence stratigraphy and tectonic controls. Rev Asoc Geol Argentina 63:534–548

Lanés S, Gnaedinger SC, Zavattieri AM et al (2013) Sedimentary paleoenvironment and fossil plants of the El Freno Formation (early Jurassic) in Las Leñas valley, Neuquén basin. Rev Asoc Geol Argentina 70:465–476

Legarreta L, Gulisano CA (1989) Análisis estratigráfico secuencial de la cuenca Neuquina (Triásico superior – Terciario inferior), Argentina. In: Chebli G, Spalletti L (eds) Cuenca Neuquina. Universidad Nacional de Tucumán, San Miguel de Tucuman, Ser. Corr Geol 6, pp 221–243

Legarreta L, Uliana MA (1996) The Jurassic succession in west-central Argentina: stratal patterns, sequences and paleogeographic evolution. Palaeo 120:303–330

Legarreta L, Uliana MA (1999) El Jurásico y Cretácico de la Cordillera Principal y Cuenca Neuquina. In: Caminos R (ed) Geología Argentina. Instituto de Geología y Recursos Minerales, Buenos Aires 29, pp 399–432

Legarreta L, Gulisano CA, Uliana MA (1993) Las secuencias sedimentarias jurásico-cretácicas. In: Ramos VA (ed) Geología y Recursos Naturales de Mendoza. Asociación Geológica Argentina, Buenos Aires, pp 87–114

Limarino CO, Spalletti L (2006) Paleogeography of the Upper Paleozoic basins of southern South America: an overview. J S Am Earth Sci 22:134–155

Llambías EJ (1999) Las rocas ígneas gondwánicas. 1. El magmatismo gondwánico durante el Paleozoico Superior-Triásico. In: Caminos R (ed), Geología Argentina. Instituto de Geología y Recursos Minerales, vol 29. Asociación Geológica Argentina, Buenos Aires, pp 349–363

Llambías EJ, Kleiman LE, Salvarredi JA (1993) El magmatismo Gondwánico. In: Ramos VA (ed.) Geología y Recursos Naturales de Mendoza. Instituto de Geología y Recursos Minerales 29, Asociación Geológica Argentina, Buenos Aires, pp 53–64

Llambías EJ, Leanza HA, Carbone O (2007) Evolución tectono-magmática durante el Pérmico al Jurásico Temprano en la Cordillera del Viento (37° 05′ S–37° 15′ S): Nuevas evidencias geológicas y geoquímicas del inicio de la cuenca Neuquina. Rev Asoc Geol Argent 62:217–235

Manceda R, Figueroa D (1995) Inversion of the Mesozoic Neuquén rift in the Malargüe fold-thrust belt, Mendoza, Argentina. In: Tankard AJ, Suárez R, Welsink HJ (eds) Petroleum basins of South America. AAPG Memoir 62:369–382

Marrett RA, Allmendinger RW (1990) Kinematic analysis of fault-slip data. J Struct Geol 12:973–986

Martinez Días JJ (2002) Stress field variation related to fault interaction in a reverse oblique-slip fault: the Alhama de Murcia fault, Betic Cordillera, Spain. Tectonophys 356:291–305

Mazzini A, Svensen H, Leanza HA et al (2010) Early Jurassic shale chemostratigraphy and U-Pb ages from the Neuquén Basin (Argentina): implications for the Toarcian oceanic anoxic event. Earth Planet Sci Lett 297:633–645

Mescua JF, Giambiagi LB, Bechis F (2008) Evidencias de Tectónica Extensional en el Jurásico Tardío (Kimeridgiano) del suroeste de la Provincia de Mendoza. Rev Asoc Geol Argentina 63:512–519

Mescua JF, Giambiagi LB, Ramos VA (2013) Late Cretaceous Uplift in the Malargüe fold-and-thrust belt (35° S), southern Central Andes of Argentina and Chile. Andean Geol 40:102–116

Mescua JF, Giambiagi LB, Tassara A et al (2014) Influence of pre-Andean history over Cenozoic foreland deformation: structural styles in the Malargüe fold-and-thrust belt at 35 S, Andes of Argentina. Geosphere 10:585–609

Mescua JF, Giambiagi L, Barrionuevo M et al (2016) Basement composition and basin geometry controls on upper- crustal deformation in the Southern Central Andes (30-36°S). Geol Magaz 153:945–961

Mosquera A, Ramos VA (2006) Intraplate deformation in the Neuquén Embayment. In: Kay SM, Ramos VA (eds) Evolution of an Andean margin: a tectonic and magmatic view from the Andes to the Neuquén Basin (35°–39° S latitude). Geol Soc Am, SP 407: 97–123

Mpodozis C, Ramos VA (1989) The Andes of Chile and Argentina. In: Ericksen GE, Cañas MT, Reinemund JA (eds) Geology of the Andes and its relation to hydrocarbon and energy resources. Circum-Pacific Council for Energy and Hydrothermal Resources, Earth Science Series 11, pp 59–90

Naipauer M, Tapia F, Mescua J, Farías M et al (2015) Detrital and volcanic zircon U-Pb ages from southern Mendoza (Argentina): an insight on the source regions in the northern part of the Neuquén Basin. J S Am Earth Sci 64:434–451

Nieto-Samaniego AF (1999) Stress, strain and fault patterns. J Struct Geol 21:1065–1070

Nullo F, Stephens G, Otamendi J et al (2002) El volcanismo del Terciario superior del sur de Mendoza. Rev Asoc Geol Argent 57:119–132

Nullo F, Stephens G, Combina A et al (2005) Hoja geológica 3569-III/3572-IV Malargüe, provincia de Mendoza. Servicio Geológico Minero Argentino. Instituto de Geología y Recursos Minerales, Buenos Aires

Oliveros V, González J, Espinoza M et al (2018) The early stages of the Magmatic Arc in the Southern Central Andes. In: Folguera A, Contreras Reyes E et al (eds) The evolution of the Chilean-Argentinean Andes. Springer, Cham, pp 165–190

Orts DL, Folguera A, Giménez M et al (2012) Variable structural controls through time in the Southern Central Andes (~36ºS). Andean Geol 39:220–241

Pángaro F, Ramos VA (2012) Paleozoic crustal blocks of onshore and offshore central Argentina: new pieces of the southwestern Gondwana collage and their role in the accretion of Patagonia and the evolution of Mesozoic south Atlantic sedimentary basins. Mar Petrol Geol 37:162–183

Pángaro F, Pereira M, Raggio F et al (2006) Tectonic inversion of the Huincul High, Neuquén Basin, Argentina: An Endangered Species. stratigraphic evidences of it's disappearance. In: Abstracts of the 9 Simposio Bolivariano de Exploración Petrolera en las Cuencas Subandinas, Aug 2006

Pankhurst RJ, Rapela CW, Fanning CM et al (2006) Gondwanide continental collision and the origin of Patagonia. Earth Sci Rev 76:235–257

Ramos VA (1988) Late Proterozoic-Early Paleozoic of South America—a collisional history. Episodes 11:168–174

Ramos VA (2008) Patagonia: a Paleozoic continent adrift? J S Am Earth Sci 26:235–251

Ramos VA (2010) The tectonic regime along the Andes: present-day and Mesozoic regimes. Geol J 45:2–25

Ramos VA, Kay SM (2006) Overview of the tectonic evolution of the southern Central Andes of Mendoza and Neuquén (35°–39° S latitude). In: Kay SM, Ramos VA (eds) Evolution of an Andean margin: A tectonic and magmatic view from the Andes to the Neuquén Basin (35°–39° S latitude). Geol Soc Am SP 407:1–18

Ramos VA, Jordan TE, Allmendinger W et al (1986) Paleozoic Terranes of the Central Argentine-Chilean Andes. Tectonics 5:855–880

Rapalini AE (2005) The accretionary history of southern South America from the latest Proterozoic to the Late Palaeozoic: some palaeomagnetic constraints. In: Vaughan APM, Leat PT, Pankhurst RJ (eds) Terrane Processes at the Margins of Gondwana. The Geological Society, London, SP 246, pp 305–328

Reijenstein C (1967) Estratigrafía y tectónica de la zona al Norte del río Atuel, entre los arroyos Blanco y Malo, provincia de Mendoza. Universidad de Buenos Aires, Trabajo final de Licenciatura

Riccardi AC, Damborenea SE (1993) Léxico estratigráfico de la Argentina: Jurásico. Asociación Geológica Argentina, Serie B 21, Buenos Aires, pp 470

Riccardi A, Iglesia Llanos MP (1999) Primer hallazgo de amonites en el Triásico de la Argentina. Rev Asoc Geol Argentina 54:298–300

Riccardi AC, Damborenea S, Manceñido MO et al (1988) Hettangiano y Sinemuriano marinos en Argentina. In: Abstracts of the 5 Congreso Geológico Chileno, Santiago de Chile, 8–12 Aug 1988

Riccardi AC, Damborenea S, Manceñido MO et al (1991) Hettangian and Sinemurian (Lower Jurassic) biostratigraphy of Argentina. J S Am Earth Sci 4:159–170

Riccardi AC, Damborenea SE, Manceñido MO et al (1997) Primer registro de Triásico marino fosilífero de la Argentina. Rev Asoc Geol Argent 52:228–234

Sato AM, Llambías E, Basei M et al (2015) Three stages in the Late Paleozoic to Triassic magmatism of southwestern Gondwana, and the relationships with the volcanogenic events in coeval basins. J S Am Earth Sci 63:48–69

Schiuma M, Llambías EJ (2008) New ages and chemical analysis on Lower Jurassic volcanism close to the Huincul High, Neuquén. Rev Asoc Geol Argent 63:644–652

Silvestro J, Kraemer P (2005) Evolución tecto-sedimentaria de la Cordillera Principal en el sector surmendocino a los 35° 30′ S. Faja Plegada de Malargüe. República Argentina. In: Abstracts of the 6°Congreso de Exploración y desarrollo de hidrocarburos, Mar del Plata, 15–19 November 2005

Silvestro J, Zubiri M (2008) Convergencia oblicua: modelo estructural alternativo para la Dorsal Neuquina (39° S) - Neuquén. Rev Asoc Geol Argent 63:49–64

Spagnuolo M, Litvak V, Folguera A et al (2012) Neogene magmatic expansion and mountain building processes in the southern Central Andes, 36-37° S, Argentina. J Geodyn 53:81–94

Spalletti LA (1997) Sistemas deposicionales fluvio-lacustres en el rift triásico de Malargüe (sur de Mendoza, República Argentina). A Acad Nac Cs Ex Fís Nat 49:109–124

Spalletti LA, Morel EM, Franzese JR et al (2007) Contribución al conocimiento sedimentológico y paleobotánico de la Formación El Freno (Jurásico Temprano) en el valle superior del río Atuel, Mendoza, Argentina. Ameghiniana 44:367–386

Sruoga P, Etcheverría M, Folguera A et al (2005) Hoja Geológica 3569-I Volcán Maipú, Servicio Geológico y Minero Argentino, Boletín 290, 116 p, Buenos Aires

Stipanicic PN (1969) El avance en los conocimientos del Jurásico argentino a partir del esquema de Groeber. Rev Asoc Geol Argent 24:367–388

Stipanicic PN (1979) El Triásico de Valle del río de Los Patos (provincia de San Juan). In: Turner JCM (ed) Geología Regional Argentina. Academia Nacional de Ciencias, Córdoba, pp 695–744

Teyssier C, Tikoff B, Markley M (1995) Oblique plate motion and continental tectonics. Geology 23:447–450

Tickyj H, Fernández MA, Chemale Jr F et al (2009). Granodiorita Pampa de los Avestruces, Cordillera Frontal, Mendoza: un intrusivo sintectónico de edad devónica inferior. In: Abstracts of the 14 Reunión de Tectónica, 19–23 Oct 2015

Tikoff B, Teyssier C (1994) Strain modelling of displacement-field partitioning in transpressional orogens. J Struct Geol 16:1575–1588

Tomezzoli RN (2012) Chilenia y Patagonia: un mismo continente a la deriva? Rev Asoc Geol Argent 69:222–239

Tunik MA, Lanés S, Bechis F et al (2008) Análisis petrográfico preliminar de las areniscas jurásicas tempranas en el depocentro Atuel de la cuenca Neuquina. Rev Asoc Geol Argent 63:714–727

Tunik MA, Folguera A, Naipauer M et al (2010) Early uplift and orogenic deformation in the Neuquén Basin: Constraints on the Andean uplift from U-Pb and Hf isotopic data of detrital zircons. Tectonophysics 489:258–273

Tunik MA, Giambiagi LB; Barredo S et al (2011) Caracterización petrográfica del relleno del rift de la subcuenca Atuel, provincia de Mendoza. In: Abstracts of the 18 Congreso Geológico Argentino, Neuquén, 2–6 May 2011

Twiss RJ, Unruh JR (1998) Analysis of fault slip inversions: Do they constrain stress or strain rate? J Geoph Res 103:12205–12222

Uliana M, Biddle K, Cerdán J (1989) Mesozoic extension and the formation of Argentina sedimentary basins. In: Tankard AJ, Balkwill HR (eds) Extensional tectonics and stratigraphy of the North Atlantic Margin). AAPG Memoir 46: 599–613

Uliana M, Arteaga M, Legarreta L et al (1995) Inversion structures and hydrocarbon occurrence in Argentina. In: Buchanan J, Buchanan P (eds) Basin inversion. The Geological Society, London, SP88: 211–233

Varela R, Basei MAS, González PD et al (2011) Accretion of Grenvillian terranes to the southwestern border of the Río de la Plata craton, western Argentina. Int J of Earth Sci 100:243–272

Vergani GD, Tankard J, Belotti J et al (1995) Tectonic evolution and paleogeography of the Neuquén Basin, Argentina. In: Tankard AJ, Suárez R, Welsink HJ (eds), Petroleum Basins of South America. AAPG Memoir 62:383–402

Volkheimer W (1978) Descripción Geológica de la Hoja 27b, Cerro Sosneado, provincia de Mendoza. Servicio Geológico Nacional, vol 151, Buenos Aires, p 83

von Hillebrandt A (1989) The Lower Jurassic of the Río Atuel region, Mendoza Province, Argentina. In: Abstracts of the 4º Congreso Argentino de Paleontología y Bioestratigrafía, Mendoza, vol 4, pp 39–43

Westermann GEG, Riccardi AC (1982) Ammonoid fauna from the early Middle Jurassic of Mendoza province, Argentina. J Paleontol 56:11–41

Yagupsky DL, Cristallini EO, Fantín J et al (2008) Oblique half-graben inversion of the Mesozoic Neuquén Rift in the Malargüe Fold and Thrust Belt, Mendoza, Argentina: new insights from analogue models. J Struct Geol 30:839–853

Yamaji A (2000) The multiple inverse method: a new technique to separate stresses from heterogeneous fault-slip data. J Struct Geol 22:441–452

Yamaji A (2003) Are the solution of stress inversion correct? Visualization of their reliability and the separation of stresses from heterogeneous fault-slip data. J Struct Geol 25:241–252

Yrigoyen MR (1993) Los depósitos sinorogénicos terciarios. In: Ramos VA (ed) Geología y Recursos Naturales de Mendoza. Asociación Geológica Argetina, Buenos Aires, pp 123–148

Zamora Valcarce G, Zapata TR, del Pino D et al (2006) Structural evolution and magmatic characteristics of the Agrio fold-and-thrust belt. In: Kay SM, Ramos VA (eds) Evolution of an Andean Margin: a Tectonic and Magmatic View from the Andes to the Neuquén Basin (35º-39ºS lat). Geol Soc Am, SP 407, p 125–145

Zapata TR, Folguera A (2005) Tectonic evolution of the Andean Fold and Thrust Belt of the southern Neuquén Basin, Argentina. In: Veiga GD, Spalletti LA, Howell JA, Schwarz E (eds) The Neuquén Basin, Argentina: a case study in sequence stratigraphy and basin dynamics. The Geological Society, London, SP 252, pp 37–56

Zapata TR, Brissón I, Dzelalija F (1999) The structures of the Andean fold and thrust belt in relation to basement control in the Neuquén Basin. Bol Inf Petrol 60:112–121